Int. J. Appl. Math. Comput. Sci., 2018, Vol. 28, No. 4, 649–659
DOI: 10.2478/amcs-2018-0050

A MEMORY–EFFICIENT NONINTEGER–ORDER DISCRETE–TIME STATE–SPACE MODEL OF A HEAT TRANSFER PROCESS

KRZYSZTOF OPRZĘDKIEWICZ [a,*], WOJCIECH MITKOWSKI [a]

[a]Department of Automatics and Robotics
AGH University of Science and Technology, al. Mickiewicza 30, 30-079 Kraków, Poland
e-mail: {kop,wojciech.mitkowski}@agh.edu.pl

A new, state space, discrete-time, and memory-efficient model of a one-dimensional heat transfer process is proposed. The model is derived directly from a time-continuous, state-space semigroup one. Its discrete version is obtained via a continuous fraction expansion method applied to the solution of the state equation. Fundamental properties of the proposed model, such as decomposition, stability, accuracy and convergence, are also discussed. Results of experiments show that the model yields good accuracy in the sense of the mean square error, and its size is significantly smaller than that of the model employing the well-known power series expansion approximation.

Keywords: noninteger-order systems, heat transfer equation, infinite dimensional systems, continuous fraction expansion, stability.

1. Introduction

Mathematical models of distributed parameter systems based on partial differential equations can be described in infinite dimensional state space, usually in a Hilbert one, but a Sobolev space can also be applied. This problem has been analyzed by many authors. Fundamentals were given, for example, by Pazy (1983) and Mitkowski (1991). An analysis of a hyperbolic system in a Hilbert space was presented by Bartecki (2013), while the modeling and control of heat plants were discussed, e.g., by Rauh *et al.* (2016).

The modeling of processes and phenomena which are hard to describe with the use of other tools is one of the main areas of applications of noninteger-order calculus. Noninteger models for physical phenomena were presented by many authors (e.g., Podlubny, 1999; Dzieliński *et al.*, 2010; Caponetto *et al.*, 2010; Das, 2010; Obrączka, 2014; Sierociuk *et al.*, 2015; Gal and Warma, 2016). Analysis of anomalous diffusion problems with the use of a fractional order approach and semigroup theory was made, for example, by Popescu (2010). An observability problem for fractional order systems was discussed, e.g., by N'Doye *et al.* (2013) or Kaczorek (2016), while controllability was investigated, e.g., by Balachandran (2012; 2014).

It is well known that heat transfer processes can also be modeled employing a noninteger-order approach. This problem was investigated, for example, by Baeumer *et al.* (2005), Kochubei (2011), Almeida and Torres (2011), Mitkowski (2011), Obrączka (2014) or Dlugosz and Skruch (2015).

This paper presents a proposal for a new, low order, discrete, state-space model for heat transfer processes in a one-dimensional plant. The model considered follows directly from the semigroup model given by Oprzędkiewicz and Gawin (2016) as well as Oprzędkiewicz *et al.* (2016a). It employs a new, continuous fraction expansion (CFE) based solution method proposed by Oprzędkiewicz *et al.* (2017b). The approach allows us to obtain a model accurate and significantly smaller than the analogous model using power series expansion (PSE) approximation, discussed by Oprzędkiewicz *et al.* (2017a).

The paper is organized as follows. Elementary ideas and definitions are mentioned at the beginning. Here the proposed CFE-based method of solving a discrete fractional-order (FO) state equation is also presented. Next, the discussed, experimental, infinite-order plant and its noninteger-order, semigroup model are recalled. Furthermore, the CFE based, discrete model of the

*Corresponding author

heat system considered is proposed and its elementary properties are analyzed. Finally, experimental verification of the proposed model is discussed.

2. Preliminaries

2.1. Elementary ideas. Fundamentals of fractional calculus can be found in many books (e.g., Das, 2010; Kaczorek, 2011; Ostalczyk, 2016; Podlubny, 1999). Here only some definitions necessary to explain of main results will be given.

At the beginning, the idea of Euler's gamma function will be recalled (see, e.g., Kaczorek and Rogowski, 2014).

Definition 1. (*Gamma function*)

$$\Gamma(x) = \int_0^\infty t^{x-1} e^{-t} \, \mathrm{d}t. \tag{1}$$

Next, the Mittag-Leffler function will be introduced. It is a noninteger-order generalization of the exponential function $e^{\lambda t}$ which plays a crucial role in the solution of fractional order (FO) state equations. It is defined as follows.

Definition 2. (*One parameter Mittag-Leffler function*)

$$E_\alpha(x) = \sum_{k=0}^{\infty} \frac{x^k}{\Gamma(k\alpha + 1)}. \tag{2}$$

The fractional-order, integro-differential operator is described by different definitions, given by Grünvald and Letnikov (GL definition), Riemann and Liouville (RL definition) and Caputo (C definition). Only the C definition will be employed in this paper. It is given as follows (Kaczorek, 2016).

Definition 3. (*Caputo definition of the FO operator*)

$${}_0^C D_t^\alpha f(t) = \frac{1}{\Gamma(N-\alpha)} \int_0^\infty \frac{f^{(N)}(\tau)}{(t-\tau)^{\alpha+1-N}} \, \mathrm{d}\tau, \tag{3}$$

where $N - 1 < \alpha < N$ denotes the noninteger order of operation and $\Gamma(\cdot)$ is the complete Gamma function expressed by (1).

The noninteger-order spatial derivative was given by Riesz and has the following form (see, e.g., Yang *et al.*, 2010).

Definition 4. (*Riesz definition of the FO spatial derivative*)

$$\frac{\partial^\gamma \Theta(x,t)}{\partial x^\gamma} = -r_\gamma \left({}_0D_x^\gamma + {}_x D_1^\gamma \right) \Theta(x,t), \tag{4}$$

where

$$r_\gamma = \frac{1}{2\cos(\frac{\pi\gamma}{2})}. \tag{5}$$

In (4), ${}_0D_x^\gamma$ and xD_1^γ denote left- and right-side Riemann–Liouville derivatives, defined as

$${}_0D_x^\gamma = \frac{1}{\Gamma(2-\alpha)} \frac{\partial}{\partial x} \int_0^x \frac{\Theta(\xi,t)\,\mathrm{d}\xi}{(x-\xi)^{\gamma-1}}, \tag{6}$$

$${}_xD_1^\gamma = \frac{1}{\Gamma(2-\alpha)} \frac{\partial}{\partial x} \int_x^1 \frac{\Theta(\xi,t)\,\mathrm{d}\xi}{(\xi-x)^{\gamma-1}}. \tag{7}$$

For the Caputo operator, the Laplace transform can be defined (see, e.g., Kaczorek, 2011).

Definition 5. (*Laplace transform for the Caputo operator*)

$$\begin{gathered} \mathcal{L}({}_0^C D_t^\alpha f(t)) = s^\alpha F(s), \quad \alpha < 0, \\ \mathcal{L}({}_0^C D_t^\alpha f(t)) = s^\alpha F(s) - \sum_{k=0}^{n-1} s^{\alpha-k-1} {}_0D_t^k f(0), \\ \alpha > 0, \quad n-1 < \alpha \le n \in \mathbb{N}. \end{gathered} \tag{8}$$

A fractional-order linear multiple-input multiple-output (MIMO) state-space system, employing the C definition, is described as follows:

$$\begin{aligned} {}_0^C D_t^\alpha x(t) &= Ax(t) + Bu(t), \\ y(t) &= Cx(t), \end{aligned} \tag{9}$$

where $\alpha \in (0,1)$ denotes the fractional order of the state equation, $x(t) \in \mathbb{R}^N$, $u(t) \in \mathbb{R}^L$, $y(t) \in \mathbb{R}^P$ are the state, control and output vectors, respectively, A, B, C are the state, control and output matrices, respectively. In this paper, the single-input, multiple-output (SIMO) system will be discussed. It is determined by the construction of the experimental system considered.

2.2. CFE approximation. In practice, an implementation of the operator s^α on each digital platform (PLC, microcontroller) requires the employment of its integer-order, finite-length, discrete-time approximator. Typical approximators are based on PSE and CFE approximations. They allow us to express a noninteger-order element in the form of digital FIR or IIR filters. The PSE approximator is based directly on a discrete-time version of the GL definition and takes the form of an FIR filter containing zeros only. However, its digital, high quality implementation requires application of a long memory buffer (a high order of the filter).

The CFE approximator has the form of an IIR filter containing both poles and zeros. It converges faster and is easier to implement because its order is relatively low, typically not higher than 5. It is obtained via discretization of the elementary fractional order element s^α. This can be done using the so-called generating function $s \approx \omega(z^{-1})$.

The new operator raised to the power α has the following form (see, e.g., Chen and Moore, 2002; Petras, 2009a):

$$\begin{aligned}&\big(\omega(z^{-1})\big)^{\alpha}\\&=g_h\mathrm{CFE}\Big\{\left(\frac{1-z^{-1}}{1+az^{-1}}\right)^{\alpha}\Big\}_{M,M}\\&=\frac{P_{\alpha M}(z^{-1})}{Q_{\alpha M}(z^{-1})}=g_h\frac{\mathrm{CFE}_N(z^{-1},\alpha)}{\mathrm{CFE}_D(z^{-1},\alpha)}\\&=g_h\frac{\sum_{m=0}^{M}w_m z^{-m}}{\sum_{m=0}^{M}v_m z^{-m}},\end{aligned}\tag{10}$$

where M is the approximation order, g_h is the coefficient depending on the sample time and the type of approximation,

$$g_h=\left(\frac{1+a}{h}\right)^{\alpha}.\tag{11}$$

In (11), h is the sample time and a is the coefficient depending on the approximation type. For $a=0$ and $a=1$, we obtain the Euler and Tustin approximations, respectively. For $a\in(0,1)$, we arrive at the Al-Alaoui based approximation, which is a linear combination of the Euler and Tustin formulas. Note that in this case the parameter a in Eqn. (10) is equal to

$$a=\frac{1-\gamma}{1+\gamma},$$

with γ being the Al-Alaoui weighting coefficient (Al-Alaoui, 1993; Stanisławski *et al.*, 2015). Numerical values of coefficients w_m and v_m and various values of the parameter a can be calculated with the use of the MATLAB function written by Petras (2009b). If the Tustin approximation is considered ($a=1$), then $\mathrm{CFE}_D(z^{-1},\alpha)=\mathrm{CFE}_N(z^{-1},-\alpha)$ and the polynomial $\mathrm{CFE}_D(z^{-1},\alpha)$ can be given in the direct form (see Chen and Moore, 2002). Examples of the polynomial $\mathrm{CFE}_D(z^{-1},\alpha)$ for $M=1,3,5$ are given in Table 1. A detailed analysis of various forms of CFE approximators is presented by Stanisławski *et al.* (2015).

Table 1. Coefficients of CFE polynomials $CFE_{N,D}(z^{-1},\alpha)$ for Tustin approximation.

Order M	w_m	v_m
$M=1$	$w_1=-\alpha$ $w_0=1$	$v_1=\alpha$ $v_0=1$
$M=3$	$w_3=-\frac{\alpha}{3}$ $w_2=\frac{\alpha^2}{3}$ $w_1=-\alpha$ $w_0=1$	$v_3=\frac{\alpha}{3}$ $v_2=\frac{\alpha^2}{3}$ $v_1=\alpha$ $v_0=1$
$M=5$	$w_5=-\frac{\alpha}{5}$ $w_4=\frac{\alpha^2}{5}$ $w_3=-\left(\frac{\alpha}{5}+\frac{2\alpha^3}{35}\right)$ $w_2=\frac{2\alpha^2}{5}$ $w_1=-\alpha$ $w_0=1$	$v_5=\frac{\alpha}{5}$ $v_4=\frac{\alpha^2}{5}$ $v_3=-\left(\frac{-\alpha}{5}+\frac{-2\alpha^3}{35}\right)$ $v_2=\frac{2\alpha^2}{5}$ $v_1=\alpha$ $v_0=1$

2.3. CFE based method of solving an FO state equation.

A method for a memory-effective solution of a state equation was proposed and analyzed by Oprzędkiewicz *et al.* (2017b). Its idea consists in replacing the continuous operator s^{α} in the Laplace transform of the FO state equation (9) by its discrete CFE approximant expressed by (10), with coefficients given in Table 1. The CFE approximant is a function of discrete complex variable z^{-1}. This allows us to directly pass on to the discrete time domain. Then the solution of the state equation takes the following form:

$$\begin{aligned}&\sum_{m=0}^{M}E_m x^{+}(k-m)\\&\qquad=\sum_{m=0}^{M}F_m u^{+}(k-m)+\sum_{m=-M}^{0}x_0(m),\end{aligned}\tag{12}$$

where matrices E_m and F_m are defined as follows:

$$\begin{cases}E_m=g_h w_m I_{N\times N}-v_m A,\\F_m=v_m B,\\m=0,1,\dots,M.\end{cases}\tag{13}$$

In (13) g_h is described by (11), and w_m and v_m denote coefficients of the CFE approximant given in Table 1. From (12), the state vector x^{+} can be directly calculated as follows:

$$\begin{aligned}x^{+}(k)=&-E_0^{-1}\sum_{m=1}^{M}E_m x^{+}(k-m)\\&+E_0^{-1}\sum_{m=0}^{M}F_m u^{+}(k-m)\\&+E_0^{-1}\sum_{m=-M}^{0}x_0(m).\end{aligned}\tag{14}$$

Equation (14) allows us to solve the discrete-time FO state equation using the CFE approximant. It has the form of an M-th order difference equation. Its solution requires the knowledge of M previous steps of state and control signals.

The state equation (12) can also be written in the extended form

$$\begin{cases}x_q^{+}(k+1)=A_q^{+}x_q^{+}(k)+B_q^{+}u_q^{+}(k),\\y_q^{+}(k)=C_q^{+}x_q^{+}(k),\end{cases}\tag{15}$$

where

$$x_q^+(k) = \begin{bmatrix} x_1^+(k) \\ x_2^+(k) \\ \vdots \\ x_M^+(k) \end{bmatrix}_{MN\times 1}, \tag{16}$$

$$\begin{cases} x_1^+(k) = x(k), \\ x_2^+(k) = x(k-1), \\ \vdots \\ x_M^+(k) = x(k+1-M). \end{cases} \tag{17}$$

$$u_q^+(k) = \begin{bmatrix} u_1^+(k) \\ u_2^+(k) \\ \vdots \\ u_{M+1}^+(k) \end{bmatrix}_{M+1\times 1}, \tag{18}$$

$$\begin{cases} u_1^+(k) = u(k), \\ u_2^+(k) = u(k-1), \\ \vdots \\ u_{M+1}^+(k) = u(k-M), \end{cases} \tag{19}$$

$$A_q^+ = \begin{bmatrix} -E_0^{-1}E_1, \dots, -E_0^{-1}E_M \\ I_{N\times N}, 0, 0, \dots, 0 \\ 0, I_{N\times N}, 0, \dots, 0 \\ \vdots \\ 0, \dots, I_{N\times N}, 0 \end{bmatrix}_{MN\times MN}, \tag{20}$$

$$B_q^+ = \begin{bmatrix} E_0^{-1}F_0, \dots, E_0^{-1}F_M \\ 0, 0, 0, \dots, 0 \\ \vdots \\ 0, 0, 0, \dots, 0 \end{bmatrix}_{MN\times M+1}. \tag{21}$$

The output matrix is

$$C_q^+ = \begin{bmatrix} C^+, 0, \dots, 0 \end{bmatrix}_{N\times MN}. \tag{22}$$

The initial condition for the state equation (15) also takes the extended form

$$x_{q0}^+ = \begin{bmatrix} x^+(M-1) \\ x^+(M-2) \\ \vdots \\ x^+(0) \end{bmatrix}_{MN\times 1}. \tag{23}$$

Notice that the summarized size of the proposed discrete, FO model is NM. This size is significantly lower than that of the model using PSE approximation, analysed by Oprzędkiewicz *et al.* (2017a).

2.4. Stability. Stability of the discrete system considered will be analyzed with the use of the approach presented by Stanislawski and Latawiec (2013a; 2013b), Ostalczyk (2016, pp. 202–223) and Oprzędkiewicz *et al.* (2017b). Its idea consists in testing the location of the spectrum of the continuous system (before its discretization) in the complex plane with respect to a restricted area, limited by the form of the CFE approximant (10). Let us assume that the approximation $\omega(z^{-1})$ of (10) is stable and the term $\omega(e^{-j\varphi})$, $\varphi \in [-\pi, \pi]$, draws a simply closed curve in the complex plane. Then the stability/instability areas with respect to the spectrum of the continuous system are separated from each other by the contour defined as follows (Stanisławski and Latawiec, 2013a; Ostalczyk, 2016, Theorem 7.4, p. 205):

$$S = \{\omega(e^{-j\varphi}), \varphi \in [-\pi, \pi]\}, \tag{24}$$

where

$$\omega(e^{-j\varphi}) = g_h \frac{\sum_{m=0}^{M} w_m (e^{-j\varphi})^m}{\sum_{m=0}^{M} v_m (e^{-j\varphi})^m}. \tag{25}$$

An example of stability/instability areas for the discrete-time approximator (10) and different ranges of order α is given in Fig. 1. In each case, the "restricted" area is located inside the contour S.

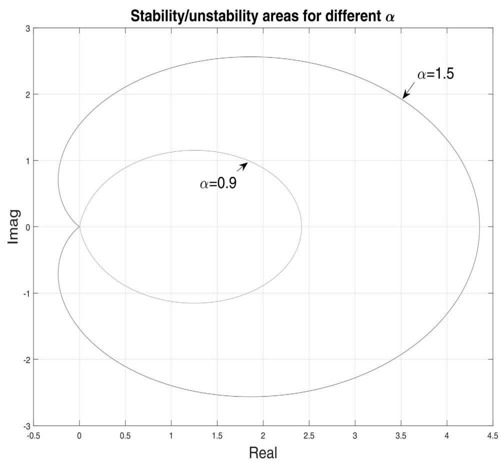

Fig. 1. Stability/unstability areas for $\alpha = 0.9, \alpha = 1.5$, $a = 1/7$, $h = 1$ [s], $M = 5$.

It is important to note that

- for $0.0 < \alpha < 1.0$, the restricted area is located in the right half-plane only,
- for $1.0 < \alpha < 2.0$ the restricted area is located in both the half-planes, but it does not cover the negative part of the real axis.

The above remarks will be fundamental during stability analysis for the discussed model of the heat plant. This is caused by the fact that the spectrum of the heat system considered has a unique location in the complex plane.

3. Noninteger-order state-space model of the heat plant

A simplified scheme of the heat plant considered is shown in Fig. 2. It has the form of a thin copper rod heated by an electric heater of length Δx_u located at one end of the rod. An output temperature is measured with the use of Pt-100 RTD sensors Δx long attached at points with coordinates 0.29, 0.50 and 0.73 of the rod length. The construction of the whole experimental system is described in detail in Section 5.

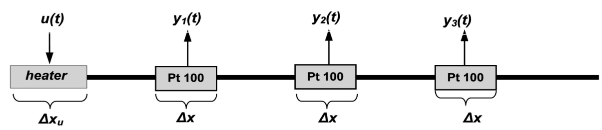

Fig. 2. Simplified scheme of the experimental system.

A fundamental mathematical model describing heat conduction in a plant is the partial differential equation of the parabolic type with homogeneous Neumann boundary conditions at the ends, the homogeneous initial condition, a heat exchange along the rod as well as distributed control and observation. This equation with integer orders of both differentiation operators has been discussed by many authors (e.g., Oprzedkiewicz, 2003; 2004; 2005). The presented, noninteger-order model is expected to describe the processes running in the plant more accurately than the integer-order model. Assume that the noninteger-order difference with respect to time is described by the Caputo definition (3) and the noninteger-order difference with respect to the length is described by the Riesz definition (4). Then the noninteger-order heat transfer equation takes the following form:

$$\begin{cases} {}^C D_t^{\alpha} Q(x,t) = a_w \dfrac{\partial^{\beta} Q(x,t)}{\partial x^{\beta}} \\ \qquad\qquad - R_a Q(x,t) + b(x)u(t), \\ \dfrac{\partial Q(0,t)}{\mathrm{d}x} = 0, \quad t \geq 0, \\ \dfrac{\partial Q(1,t)}{\partial x} = 0, \quad t \geq 0, \\ Q(x,0) = 0, \quad 0 \leq x \leq 1, \\ y(t) = y_0 \int_0^1 Q(x,t)c(x)\,\mathrm{d}x, \end{cases} \tag{26}$$

where $\alpha, \beta > 0$ denote noninteger orders of the system, and a_w, and R_a denote the coefficients of heat conduction and heat exchange, respectively.

Now we need to express (26) as an inifinte dimensional state equation in the Hilbert space, analogically as presented by Oprzędkiewicz *et al.* (2016a). The proposed state equation is written as follows:

$$\begin{cases} {}^C D_t^{\alpha} Q(t) = AQ(t) + Bu(t), \\ Q(0) = 0, \\ y(t) = y_0 CQ(t), \end{cases} \tag{27}$$

where

$$\begin{cases} AQ(x) = a_w \dfrac{\partial^{\beta} Q(x)}{\partial x^{\beta}} - R_a Q(x), \\ D(A) = \left\{ Q \in H^2(0,1) : Q'(0) = 0, Q'(1) = 0 \right\}, \\ a_w, R_a > 0, \\ H^2(0,1) = \left\{ u \in L^2(0,1) : u', u'' \in L^2(0,1) \right\}, \\ CQ(t) = \langle c, Q(t) \rangle, \quad Bu(t) = bu(t) \\ Q(t) = [q_1(t), q_2(t), \dots]^T. \end{cases} \tag{28}$$

The following set of the eigenvectors for the state operator A forms an orthonormal basis of the state space:

$$h_n = \begin{cases} 1, & n = 0, \\ \sqrt{2}\cos(n\pi x), & n = 1, 2, \dots. \end{cases} \tag{29}$$

The eigenvalues of the state operator are expressed as

$$\lambda_{\beta_n} = -a_w \pi^{\beta} n^{\beta} - R_a, \quad n = 0, 1, 2, \dots, \tag{30}$$

and, consequently, the state operator has the form

$$A = \mathrm{diag}\{\lambda_{\beta_0}, \lambda_{\beta_1}, \lambda_{\beta_2}, \dots\}. \tag{31}$$

Next, the spectrum σ of the state operator A is expressed as

$$\sigma(A) = \{\lambda_{\beta_0}, \lambda_{\beta_1}, \lambda_{\beta_2}, \dots\}. \tag{32}$$

The input operator B has the form

$$B = [b_0, b_1, b_2, \dots]^T, \tag{33}$$

where $b_n = \langle b, h_n \rangle$, and $b(x)$ denotes the shaping function

$$b(x) = \begin{cases} 1, & x \in [0, x_0], \\ 0, & x \notin [0, x_0]. \end{cases} \tag{34}$$

With respect to (29) and (34), each element b_n takes the following form:

$$b_n = \begin{cases} x_u, & n = 0, \\ \dfrac{\sqrt{2}\sin(n\pi x_u)}{n\pi}, & n = 1, 2, \dots. \end{cases} \tag{35}$$

The output operator C is expressed as follows:

$$C = \begin{bmatrix} C_{s1} \\ C_{s2} \\ C_{s3} \end{bmatrix}. \tag{36}$$

The rows of C are

$$C_{sj} = [c_{sj,0}, c_{sj,1}, c_{sj,2}, \dots], \quad j = 1, 2, 3, \dots \tag{37}$$

where $c_{sj,n} = \langle c, h_n \rangle$, and $c(x)$ denotes the output sensor function:

$$c(x) = \begin{cases} 1, & x \in [x_1, x_2], \\ 0, & x \notin [x_1, x_2]. \end{cases} \tag{38}$$

With respect to (29) and (38), each element c_{jn} takes the form

$$c_{jn} = \begin{cases} x_{j2} - x_{j1}, & n = 0, \\ \dfrac{\sqrt{2}\,(\sin(n\pi x_{j2}) - \sin(n\pi x_{j1}))}{n\pi}, & n = 1, 2, \dots, \\ & j = 1, 2, 3. \end{cases} \tag{39}$$

Coordinates x_1 and x_2 depend on the sensor locations. Their values for the experimental system considered are given in the Section 5.

The solution of state equation (27) can be calculated using the Laplace transform for the Caputo operator on the assumption that the initial condition is to zero, i.e., $Q(x, 0) = 0$ for $0 \le x \le 1$, and state and control operators are described by (31)–(35). If we assume that the control signal has the form of the Heaviside function $u(t) = 1(t)$, then the solution is as follows:

$$y_j(t) = y_{0_j} \sum_{n=0}^{\infty} \frac{(E_\alpha(\lambda_{\beta_n} t^\alpha) - 1(t))}{\lambda_{\beta_n}} \langle b, h_n \rangle \langle c, h_n \rangle, \tag{40}$$

$j = 1, 2, 3$. Consequently, the system output is

$$y(t) = [y_1(t), y_2(t), y_3(t)]^T. \tag{41}$$

Note that for the orders $\alpha = 1$ and $\beta = 2$ the proposed noninteger-order model described by (26)–(40) turns into an integer-order model. Next, the noninteger-order model described by (27)–(40) is an infinite dimensional model. Its practical usefulness requires application of its finite dimensional approximation. This can be obtained by truncating further modes in the state equation (27) and consequently calculating the solutions (40) and (41) as a finite sum expressed by (42). Consequently, operators A, B and C can be interpreted as matrices and the solution (40) becomes the following finite sum:

$$y_j(t) = y_{0_j} \sum_{n=0}^{N} \frac{(E_\alpha(\lambda_{\beta_n} t^\alpha) - 1(t))}{\lambda_{\beta_n}} \langle b, h_n \rangle \langle c, h_n \rangle, \tag{42}$$

$j = 1, 2, 3$. In (42), N denotes the order of finite approximation. Its correct estimation is an important problem while using the presented model. The value of N can be estimated numerically, as presented by Oprzędkiewicz *et al.* (2016b).

4. Main results

4.1. Time-discrete, noninteger-order, state-space model of the heat plant. The discrete state equation (14) for the model (27) takes the form

$$\begin{aligned} Q^+(k) &= -E_0^{-1} \sum_{m=1}^{M} E_m Q^+(k-m) \\ &\quad + E_0^{-1} \sum_{m=0}^{M} F_m u^+(k-m) \\ &\quad + E_0^{-1} \sum_{m=-M}^{0} q_0(m). \end{aligned} \tag{43}$$

The state vector has the form $Q^+(k) = [q_1^+(k), q_2^+(k), \dots]^T$, matrices $-E_0^{-1}E_m$ in (43) with respect to (31) and (30) take the form

$$\begin{aligned} E_m^+ &= E_0^{-1} E_m \\ &= \mathrm{diag}\{e_{1m}, \dots, e_{Nm}\}, \quad m = 1, \dots, M, \end{aligned} \tag{44}$$

where

$$e_{nm} = \frac{g_h w_m + v_m (a_w n^\beta \pi^\beta + R_a)}{v_0 (a_w n^\beta \pi^\beta + R_a)} \tag{45}$$

and, similarly,

$$\begin{aligned} F_m^+ &= E_0^{-1} F_m \\ &= [f_{1m}, \dots, f_{Nm}]^T, \quad m = 1, \dots, M, \end{aligned} \tag{46}$$

where

$$f_{nm} = \frac{v_m b_n}{v_0 (a_w n^\beta \pi^\beta + R_a)}. \tag{47}$$

The discrete system (43)–(47) can be expressed also in the first-order extended form (15)–(23). The matrices A_q^+, B_q^+ and C_q^+ for the expanded system (15) are obtained using (45) and (47). The extended system is easy to use during simulations because it can be solved with the use of standard tools available on the MATLAB platform.

4.2. Decomposition of the system. The form of the discrete equation (43) with the matrices (44) and (46) implies the possibility of its decomposition, in much the same way as this was done for the time-continuous case. The n-th mode of the solution for the decomposed system is expressed as follows:

$$q_n^+(k) = \sum_{m=1}^{M} e_{nm} q_n^+(k-m) + \sum_{m=0}^{M} f_{nm} u^+(k-m). \tag{48}$$

The discrete transfer function $G_n^+(z^{-1})$ of the n-th mode is

$$G_n^+(z^{-1}) = \frac{c_{jn}\sum\limits_{m=1}^{M} f_{nm}z^{-m}}{1-\sum\limits_{m=1}^{M} e_{nm}z^{-m}}, \tag{49}$$

where e_{nm} and f_{nm} are expressed by (45) and (47), respectively. The characteristic polynomial associated with the n-th mode of the solution (48) has the following form:

$$w_n^+(z^{-1}) = 1 - \sum_{m=1}^{M} e_{nm}z^{-m}. \tag{50}$$

The steady-state response of the n-th mode y_{jn}^{ss} can be obtained with the use of the final-value theorem (FVT) for discrete systems. If the control signal is the Heaviside function $u(k) = 1(k)$ then y_{jn}^{ss} is as follows:

$$y_{jn}^{ss} = \frac{c_{jn}\sum\limits_{m=1}^{M} f_{nm}}{1-\sum\limits_{m=1}^{M} e_{nm}} = \frac{Fc_{jn}b_n}{\lambda_{\beta_n}(F-\lambda_{\beta_n})}, \tag{51}$$

where F is expressed as

$$F = \frac{\sum_{m=0}^{M} w_m}{\sum_{m=0}^{M} v_m}. \tag{52}$$

In (52), w_m and v_m denote the coefficients of CFE approximation, given in Table 1.

With respect to (35), (39) and some elementary transformations, we obtain the direct dependency between the steady-state response of the n-th mode and parameters of the plant:

$$y_{jn}^{ss} = \frac{4}{(F-\lambda_{\beta_n})\pi^2n^2}\sin\left(\frac{n\pi(x_{j2}-x_{j1})}{2}\right) \cdot\cos\left(\frac{n\pi(x_{j2}+x_{j1})}{2}\right)\sin\left(\frac{n\pi x_u}{2}\right). \tag{53}$$

4.3. Stability. The stability of the proposed discrete model was analysed using the frequency approach presented in Section 2.4. It is described by the following proposition.

Proposition 1. (Asymptotic stability of the discrete CFE model) *Consider the discrete model of a heat transfer process described by* (27)–(37) *with a noninteger order* $0.0 < \alpha < 2.0$ *and its discrete CFE based approximation* (43). *The discrete approximation* (43) *is asymptotically stable for the fractional order* $0.0 < \alpha < 2.0$*, and each approximation order* M*, sample time* h *and weight parameter* a*.*

Proof. The spectrum $\sigma(A)$ of the heat plant considered, cf. (32), contains negative, single, separated, purely real eigenvalues. All these eigenvalues are located in the left half-plane, on the real axis.

Stability areas for the discrete, fractional order system described by the CFE approximation and different ranges of order α are given in Fig. 1. From this figure it can be noted immediately that

- the unstability area expressed by (24) for $0.0 < \alpha < 1.0$ is located in the right half-plane, and for each M, h and a it does not exceed the imaginary axis;
- the unstability area expressed by (24) for $1.0 < \alpha < 2.0$ is located in both half-planes, but for each M, h and a it does not cover the negative part of the real axis.

The above observations allow us to conclude that, for $0.0 < \alpha < 2.0$ and each set of the other approximation parameters M, h and s, the spectrum $\sigma(A)$ is located outside the unstability area. This completes the proof. ■

4.4. Accuracy. The accuracy of the model we deal with can be estimated using the approach presented by Oprzędkiewicz *et al.* (2017b) with the use of the steady-state error of the model considered. This error can be estimated using Proposition 1 by Oprzędkiewicz *et al.* (2017b):

$$\epsilon_{ss} = C\big(F-A\big)^{-1}FA^{-1}Bu_{ss} = [\epsilon_{ss1}, \epsilon_{ss2}, \epsilon_{ss3}]^T, \tag{54}$$

where u_{ss} is the steady-state value of the control signal and F is defined by (52). The steady-state error given by (54) has the form of a vector. Each component of this vector describes an error of a suitable output. If the control is the Heaviside function $u(t) = 1(t)$, then the steady-state error at the j-th output ($j = 1, 2, 3$) takes the following form:

$$\epsilon_{ssj} = F\sum_{n=0}^{N}\frac{c_{jn}b_n}{\lambda_{\beta_n}(F-\lambda_{\beta_n})}, \tag{55}$$

where λ_{β_n}, b_n and c_{jn} are described by (30), (35) and (39), respectively.

4.5. Convergence. The convergence analysis can be performed by estimating order N assuring a predefined value of the rate of convergence (ROC). In the case considered the ROC can be defined as the increment in the steady-state response y_{jn}^{ss} as a function of the order N. This increment can be defined as the absolute value of the N-th mode of the steady-state response:

$$\mathrm{ROC}_N = |y_{jN}^{ss}|, \tag{56}$$

where y_{jn}^{ss} is expressed by (51) and (53). The order N assuring keeping the predefined value Δ_N of ROC_N is characterized by the following proposition:

Proposition 2. (Model order N guaranteeing a predefined value Δ_N by the ROC) *Consider the discrete model of heat transfer process described by* (27)–(37) *with a non-integer order* $0.0 < \alpha < 2.0$ *and its discrete, CFE based approximation* (43). *Let the ROC of the discrete approximated model be defined by* (56). *The order N of the model guaranteeing a predefined value* Δ_N *of* ROC_N *meets the following inequality:*

$$N \geq \sqrt{\frac{-(F+R_a)+\sqrt{(F+R_a)^2+\frac{16a_w}{\Delta_N}}}{\pi^2 a_w}}. \quad (57)$$

Proof. The condition $\text{ROC}_N \leq \Delta_N$ is equivalent to

$$\Delta_N \geq \left|\frac{4}{(F-\lambda_{\beta_N})\pi^2 N^2}\right| \cdot P, \quad (58)$$

where

$$P = \left|\sin\left(\frac{N\pi(x_{j2}-x_{j1})}{2}\right)\cos\left(\frac{N\pi(x_{j2}+x_{j1})}{2}\right) \cdot \sin\left(\frac{N\pi x_u}{2}\right)\right|. \quad (59)$$

Notice that P expressed by (59) is not greater than one, which allows us to assume that P is equal to one. It will give us an upper estimate of N, but (58) takes a much simpler form

$$\left|\frac{4}{(F-\lambda_{\beta_N})\pi^2 N^2}\right| \leq \Delta_N. \quad (60)$$

Using (30), we rewrite (60) as

$$\left|\frac{4}{(F+a_w\pi^\beta N^\beta+R_a)\pi^2 N^2}\right| \leq \Delta_N. \quad (61)$$

The expression inside the absolute value is always positive. Consequently, the absolute value can be ignored:

$$\frac{4}{(F+a_w\pi^\beta N^\beta+R_a)\pi^2 N^2} \leq \Delta_N. \quad (62)$$

The left-hand side of (62) will be called the noninteger-order limiter $L_{\text{nio}}(N)$:

$$L_{\text{nio}}(N) = \frac{4}{(F+a_w\pi^\beta N^\beta+R_a)\pi^2 N^2}. \quad (63)$$

Next, assume that $\beta = 2$ (we consider an integer-order model with respect to length). Then the noninteger-order limiter (63) takes its integer-order form $L_{io}(N)$:

$$L_{io}(N) = \frac{4}{(F+a_w\pi^2 N^2+R_a)\pi^2 N^2}. \quad (64)$$

Consequently, the inequality (62) turns into

$$\Delta_N\pi^4 a_w N^4 + \Delta_N\pi^2(F+R_a)N^2 - 4 \geq 0. \quad (65)$$

The solution of the double quadratic inequality (65) gives directly the condition (57). This ends the proof. ∎

The condition (57) gives only an upper estimate of N, but for decreasing values of Δ_N the accuracy of the proposed estimate increases. This will be shown in an example.

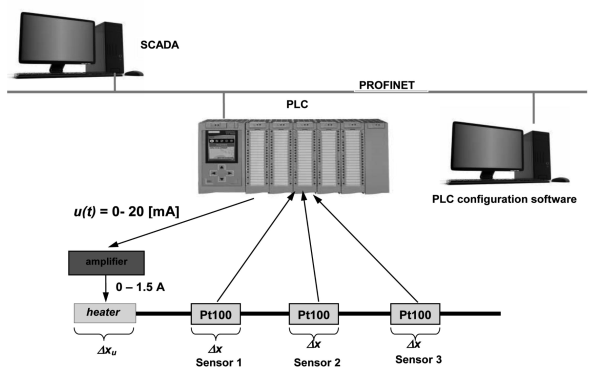

Fig. 3. Construction of the experimental system.

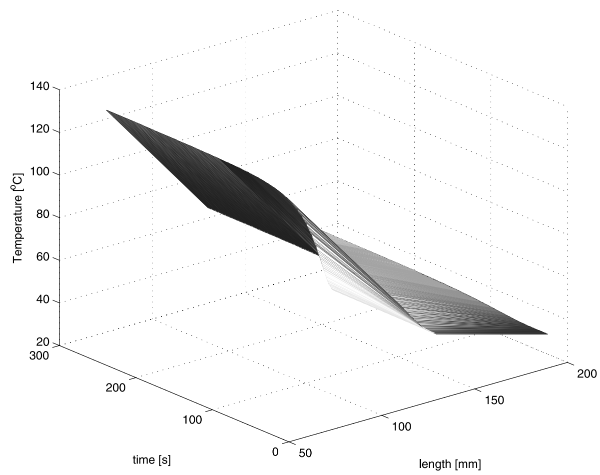

Fig. 4. Spatiotemporal temperature distribution in the plant.

5. Experimental results

Experiments have been executed using the experimental system shown in Fig. 3. The length of the rod is equal to 260 [mm]. The control signal in the system is the standard current in the range from 0 to 20 [mA] provided by the analogue output of the PLC. Next, it is amplified to the range from 0 to 1.5 [A] and sent to the electric heater of length $\Delta x_0 = 0.14$ attached at the end of the rod. The output temperature is measured by RTD sensors Pt100

Table 2. Model parameters.

α	β	a_w	R_a	a	M	N	MSE (66)
0.9402	2.2054	0.0007	0.0336	0.7215	5	8	0.1366

Table 3. Steady state error ϵ_{ss} for different N and all outputs.

N	8	15	25
ϵ_{ss1}	-0.0404	-0.0405	-0.0406
ϵ_{ss2}	-0.0173	-0.0172	-0.0172
ϵ_{ss3}	-0.0045	-0.0043	-0.0043

long $\Delta x = 0.06$ located at points with coordinates 0.29, 0.50 and 0.73 of the rod length.

Signals from the sensors are directly read by analogue inputs of the PLC in degrees Celsius. Data from PLC are read and archivized by SCADA. The whole system is connected via PROFINET. The temperature distribution with respect to time and length is shown in Fig. 4. The step response of the model was tested in the time range from 0 to $T_f = 300$ [s] with sampling time $h = 1$ [s], and the physical range of the step control signal was between 8.0 and 12.0 [mA].

Model parameters were calculated via minimization of the mean square error (MSE) cost function (66) using the function *fminsearch* from MATLAB,

$$\text{MSE} = \frac{1}{3K_s}\sum_{j=1}^{3}\sum_{k=1}^{K_s} e_j^+(k). \tag{66}$$

The results are given in Table 2. In (66), K_s denotes the number of collected samples for one sensor, $e_j^+(k)$ is the difference between the responses of the model and the plant at the k-th time moment and at the j-th output:

$$e_j^+(k) = y_{p_j}^+(k) - y_j^+(k). \tag{67}$$

The step response of the model compared with the step response of the plant is given in the Fig. 5.

Next, the accuracy of the proposed model was estimated using the steady state errors (54) and (55). The results are given in Table 3.

It can be noted that the steady state accuracy of the proposed model practically does not depend on the order N.

Finally, convergence has been tested using Proposition 2. The predefined value of the ROC was $\Delta_N = 0.001$. Using condition (56), we obtain $N = 15$. A comparison of the limiters (63) and (64) with steady-state values of the modes (53) is drawn in Fig. 6. It can be noted that use of the noninteger-order limiter gives the exact estimate $N = 13$, which is slightly better than the integer-order estimate introduced by Proposition 2.

6. Conclusions

The proposed fractional order, discrete, finite dimensional model of a heat process assures good accuracy in the sense of the MSE cost function. Simultaneously, the summarized order of the model is relatively low in contrast to the model employing PSE approximation which has previously been discussed by the same authors. Some fundamental properties of the model (spectrum decomposition, stability, accuracy and convergence) were also discussed. The presented results can be generalized to other fractional-order systems possible provided that they are characterized by a diagonal state operator (for example, in Jordan canonical form).

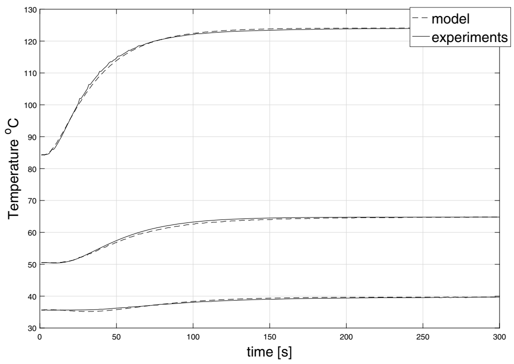

Fig. 5. Comparison of the experiment with the model parameters given in Table 2.

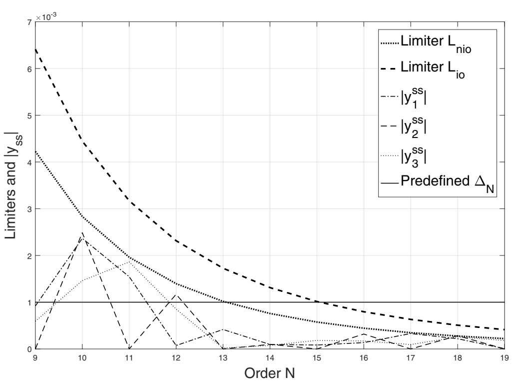

Fig. 6. Convergence estimation for $\Delta_N = 0.001$ and the model parameters given in Table 2.

Acknowledgment

This work was supported by the AGH UST project no. 11.11.120.817.

References

Al-Alaoui, M. (1993). Novel digital integrator and differentiator, *Electronics Letters* **29**(4): 376–378.

Almeida, R. and Torres, D.F.M. (2011). Necessary and sufficient conditions for the fractional calculus of variations with Caputo derivatives, *Communications in Nonlinear Science and Numerical Simulation* **16**(3): 1490–1500.

Rauh, A., Senkel, L., Aschemann, H., Saurin, V.V. and Kostin, G.V. (2016). An integrodifferential approach to modeling, control, state estimation and optimization for heat transfer systems, *International Journal of Applied Mathematics and Computer Science* **26**(1): 15–30, DOI: 10.1515/amcs-2016-0002.

Baeumer, B., Kurita, S. and Meerschaert, M. (2005). Inhomogeneous fractional diffusion equations, *Fractional Calculus and Applied Analysis* **8**(4): 371–386.

Balachandran, K. and Divya, S. (2014). Controllability of nonlinear implicit fractional integrodifferential systems, *International Journal of Applied Mathematics and Computer Science* **24**(4): 713–722, DOI: 10.2478/amcs-2014-0052.

Balachandran, K. and Kokila, J. (2012). On the controllability of fractional dynamical systems, *International Journal of Applied Mathematics and Computer Science* **22**(3): 523–531, DOI: 10.2478/v10006-012-0039-0.

Bartecki, K. (2013). A general transfer function representation for a class of hyperbolic distributed parameter systems, *International Journal of Applied Mathematics and Computer Science* **23**(2): 291–307, DOI: 10.2478/amcs-2013-0022.

Caponetto, R., Dongola, G., Fortuna, L. and Petras, I. (2010). Fractional order systems: Modeling and control applications, *in* L.O. Chua (Ed.), *World Scientific Series on Nonlinear Science*, University of California, Berkeley, CA, pp. 1–178.

Chen, Y.Q. and Moore, K.L. (2002). Discretization schemes for fractional-order differentiators and integrators, *IEEE Transactions on Circuits and Systems I: Fundamental Theory and Applications* **49**(3): 263–269.

Das, S. (2010). *Functional Fractional Calculus for System Identification and Control*, Springer, Berlin.

Dlugosz, M. and Skruch, P. (2015). The application of fractional-order models for thermal process modelling inside buildings, *Journal of Building Physics* **1**(1): 1–13.

Dzieliński, A., Sierociuk, D. and Sarwas, G. (2010). Some applications of fractional order calculus, *Bulletin of the Polish Academy of Sciences: Technical Sciences* **58**(4): 583–592.

Gal, C. and Warma, M. (2016). Elliptic and parabolic equations with fractional diffusion and dynamic boundary conditions, *Evolution Equations and Control Theory* **5**(1): 61–103.

Kaczorek, T. (2011). *Selected Problems of Fractional Systems Theory*, Springer, Berlin.

Kaczorek, T. (2016). Reduced-order fractional descriptor observers for a class of fractional descriptor continuous-time nonlinear systems, *International Journal of Applied Mathematics and Computer Science* **26**(2): 277–283, DOI: 10.1515/amcs-2016-0019.

Kaczorek, T. and Rogowski, K. (2014). *Fractional Linear Systems and Electrical Circuits*, Bialystok University of Technology, Bialystok.

Kochubei, A. (2011). Fractional-parabolic systems, *arXiv:*1009.4996 [math.ap].

Mitkowski, W. (1991). *Stabilization of Dynamic Systems*, WNT, Warsaw, (in Polish).

Mitkowski, W. (2011). Approximation of fractional diffusion-wave equation, *Acta Mechanica et Automatica* **5**(2): 65–68.

N'Doye, I., Darouach, M., Voos, H. and Zasadzinski, M. (2013). Design of unknown input fractional-order observers for fractional-order systems, *International Journal of Applied Mathematics and Computer Science* **23**(3): 491–500, DOI: 10.2478/amcs-2013-0037.

Obrączka, A. (2014). *Control of Heat Processes with the Use of Non-integer Models*, PhD thesis, AGH UST, Kraków.

Oprzędkiewicz, K. (2003). The interval parabolic system, *Archives of Control Sciences* **13**(4): 415–430.

Oprzędkiewicz, K. (2004). A controllability problem for a class of uncertain parameters linear dynamic systems, *Archives of Control Sciences* **14**(1): 85–100.

Oprzędkiewicz, K. (2005). An observability problem for a class of uncertain-parameter linear dynamic systems, *International Journal of Applied Mathematics and Computer Science* **15**(3): 331–338.

Oprzędkiewicz, K. and Gawin, E. (2016). A noninteger order, state space model for one dimensional heat transfer process, *Archives of Control Sciences* **26**(2): 261–275.

Oprzędkiewicz, K., Gawin, E. and Mitkowski, W. (2016a). Modeling heat distribution with the use of a noninteger order, state space model, *International Journal of Applied Mathematics and Computer Science* **26**(4): 749–756, DOI: 10.1515/amcs-2016-0052.

Oprzędkiewicz, K., Gawin, E. and Mitkowski, W. (2016b). Parameter identification for noninteger order, state space models of heat plant, *MMAR 2016: 21st International Conference on Methods and Models in Automation and Robotics, Międzyzdroje, Poland*, pp. 184–188.

Oprzędkiewicz, K., Mitkowski, W. and Gawin, E. (2017a). An accuracy estimation for a noninteger order, discrete, state space model of heat transfer process, *Automation 2017: Innovations in Automation, Robotics and Measurement Techniques, Warsaw, Poland*, pp. 86–98.

Oprzędkiewicz, K., Stanisławski, R., Gawin, E. and Mitkowski, W. (2017b). A new algorithm for a CFE approximated solution of a discrete-time noninteger-order state equation, *Bulletin of the Polish Academy of Sciences: Technical Sciences* **65**(4): 429–437.

Ostalczyk, P. (2016). *Discrete Fractional Calculus. Applications in Control and Image Processing*, World Scientific, Singapore.

Pazy, A. (1983). *Semigroups of Linear Operators and Applications to Partial Differential Equations*, Springer, New York, NY.

Petras, I. (2009a). Fractional order feedback control of a DC motor, *Journal of Electrical Engineering* **60**(3): 117–128.

Petras, I. (2009b). `http://people.tuke.sk/igor.podlubny/USU/matlab/petras/dfod2.m`.

Podlubny, I. (1999). *Fractional Differential Equations*, Academic Press, San Diego, CA.

Popescu, E. (2010). On the fractional Cauchy problem associated with a feller semigroup, *Mathematical Reports* **12**(2): 181–188.

Sierociuk, D., Skovranek, T., Macias, M., Podlubny, I., Petras, I., Dzielinski, A. and Ziubinski, P. (2015). Diffusion process modeling by using fractional-order models, *Applied Mathematics and Computation* **257**(1): 2–11.

Stanisławski, R. and Latawiec, K. (2013a). Stability analysis for discrete-time fractional-order LTI state-space systems. Part I: New necessary and sufficient conditions for asymptotic stability, *Bulletin of the Polish Academy of Sciences: Technical Sciences* **61**(2): 353–361.

Stanisławski, R. and Latawiec, K. (2013b). Stability analysis for discrete-time fractional-order LTI state-space systems. Part II: Stability criterion for FD-based systems, *Bulletin of the Polish Academy of Sciences; Technical Sciences* **61**(2): 362–370.

Stanisławski, R., Latawiec, K. and Łukaniszyn, M. (2015). A comparative analysis of Laguerre-based approximators to the Grünwald–Letnikov fractional-order difference, *Mathematical Problems in Engineering* **2015**(1): 1–10.

Yang, Q., Liu, F. and Turner, I. (2010). Numerical methods for fractional partial differential equations with Riesz space fractional derivatives, *Applied Mathematical Modelling* **34**(1): 200–218.

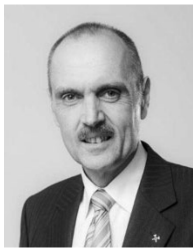

Krzysztof Oprzędkiewicz was born in Kraków in 1964. He obtained his MSc in electronics in 1988, while his PhD and DSc in his automatics and robotics in 1995 and 2009, respectively, at the AGH University (Poland). He has been working there in the Department of Automatics since 1988, recently as a professor. His research covers infinite dimensional systems, fractional order modeling and control, uncertain parameter systems, industrial automation, PLC and SCADA systems, and mobile robotics.

Wojciech Mitkowski was born in 1946 in Kraków. In 1970 he obtained an MSc in electrical engineering and automation at the Faculty of Electrical Engineering, AGH University of Science and Technology in Kraków, Poland. He has been working in this department ever since. He obtained a PhD at the same faculty in 1974, and in 1984 he was granted a DSc degree in automatics and robotics. The President of Poland awarded him with the title of a professor of technical sciences in 1992. He has been a member of the Committee on Electrical Engineering, Computer Science and Control of the Polish Academy of Sciences, Cracow Branch, since 1988. He is also a member of the Committee on Automatic Control and Robotics of the Polish Academy of Sciences (since 1996). Between 2005 and 2010 he was the head of the Kraków Branch of the Polish Mathematical Society. His research interests include automation and robotics, control theory, optimal control, dynamic systems, circuits theory, numerical methods and applications of mathematics. He has published 9 books and 238 scientific papers.

Received: 5 March 2018
Revised: 8 June 2018
Accepted: 14 July 2018